Siberian tree-ring and stable isotope proxies as indicators of temperature and moisture changes after major stratospheric volcanic eruptions

Olga V. Churakova[1,2*], Marina V. Fonti[2], Matthias Saurer[3,4], Sébastien Guillet[1], Christophe Corona[5], Patrick Fonti[3], Vladimir S. Myglan[6], Alexander V. Kirdyanov[2,7,8], Oksana V. Naumova[6], Dmitriy V. Ovchinnikov[7], Alexander Shashkin[2,7], Irina Panyushkina[9], Ulf Büntgen[3,8], Malcolm K. Hughes[9], Eugene A. Vaganov[2,7,10], Rolf T.W. Siegwolf[3,4], Markus Stoffel[1,11,12]

[1]*Institute for Environmental Sciences, University of Geneva, CH-1205 Geneva, Switzerland*

[2]*Institute of Ecology and Geography, Siberian Federal University RU-660049 Krasnoyarsk, Svobodniy pr 79/10, Russia*

[3]*Swiss Federal Institute for Forest, Snow and Landscape Research WSL, Zürcherstrasse 111, CH-8903 Birmensdorf, Switzerland*

[4]*Paul Scherrer Institute, CH- 5232 Villigen - PSI, Switzerland*

[5]*Université Blaise Pascal, Geolab, UMR 6042 CNRS, 4 rue Ledru, F-63057 Clermont-Ferrand, France*

[6]*Institute of Humanities, Siberian Federal University RU-660049 Krasnoyarsk, Svobodniy pr 82, Russia*

[7]*Sukachev Institute of Forest SB RAS, Federal Research Center "Krasnoyarsk Science Center SB RAS" RU-660036 Krasnoyarsk, Akademgorodok 50, bld. 28, Russia*

[8]*Department of Geography, University of Cambridge, Downing Place, Cambridge CB2 3EN*

[9]*Laboratory of Tree-Ring Research, University of Arizona, 1215 E. Lowell St., Tucson, 85721, USA*

[10]*Siberian Federal University, Rectorate, RU-660049 Krasnoyarsk, Svobodniy pr 79/10, Russia*

[11]*dendrolab.ch, Department of Earth Sciences, University of Geneva, 13 rue des Maraîchers, CH-1205 Geneva, Switzerland*

[12]*Department F.A. Forel for Aquatic and Environmental Sciences, University of Geneva, 66 Boulevard Carl-Vogt, CH-1205 Geneva, Switzerland*

Corresponding author: Olga V. Churakova*

E-Mail: olga.churakova@hotmail.com

Abstract

Stratospheric volcanic eruptions have far-reaching impacts on global climate and society. Tree rings can provide valuable climatic information on these impacts across different spatial and temporal scales. To detect temperature and hydro-climatic changes after strong stratospheric volcanic eruptions (535, 540, 1257, 1640, 1815, and 1991), we measured and analyzed tree-ring width (TRW), maximum latewood density (MXD), cell wall thickness (CWT), and $\delta^{13}C$ and $\delta^{18}O$ in tree-ring cellulose chronologies of climate-sensitive larch from three different Siberian regions (Northeastern Yakutia - YAK, Eastern Taimyr – TAY, and Russian Altai – ALT).

All tree-ring proxies proved to encode a significant and specific climatic signal of the growing season. Our findings suggest that TRW, MXD, and CWT show strong negative summer air temperature anomalies in 536, 541-542, and 1258-1259 at all study sites. Based on $\delta^{13}C$, 536 was extremely humid in YAK and TAY, whereas 541 was humid in ALT, but led to at least two dry summers across two Siberian sites following the 1257 eruption. No extreme hydro-climatic anomalies occurred at Siberian sites after the volcanic eruptions in 1640, 1815 and 1991. The signal stored in $\delta^{18}O$ indicated significantly lower summer sunshine duration in 536, 541-542, 1258-1259 in YAK, and 536 in ALT. These results show that trees growing at YAK and ALT mainly responded the first year after the eruptions, whereas at TAY, the growth response occurred after two years.

These different climatic responses in space and time evidence the added value of a multiple tree-ring proxies assessment to provide a more realistic picture of the impact of volcanic eruption to past climate dynamics, which is fundamental to validate global climate models.

Key words: $\delta^{13}C$ and $\delta^{18}O$ in tree-ring cellulose, tree-ring width, maximum latewood density, cell wall thickness, drought, temperature, precipitation, sunshine duration, vapor pressure deficit

1. Introduction

Major stratospheric volcanic eruptions can substantially modify the Earth's radiative balance and cool the troposphere. This is due to the massive injection of sulphate aerosols, which are able to reduce surface temperatures on timescales ranging from months to years (Robock, 2000). The cooling associated with the radiative effects of volcanic aerosols, which significantly absorb terrestrial radiation and scatter incoming solar radiation, has been estimated to about 0.5°C during the two years following the Mount Pinatubo eruption in June 1991 (Hansen et al., 1996).

Since trees – as living organisms – are impacted in their metabolism by environmental changes, their responses to these changes are recorded in the biomass, as it is found in tree-ring parameters (Schweingruber, 1996). The decoding of tree-ring archives is used to reconstruct past climates. A summer cooling of the Northern Hemisphere (NH) ranging from 0.6°C to 1.3°C has been reported after the strongest eruptions of the past 1,500 years: CE 1257 Samalas, 1452/3 Unknown, 1600 Huaynaputina, and 1815 Tambora eruptions based on tree-ring width (TRW) and maximum latewood density (MXD) reconstructions (Briffa et al., 1998; Schneider et al., 2015; Stoffel et al., 2015; Wilson et al., 2016; Esper et al., 2017; Guillet et al., 2017).

According to climate simulations, significant changes in the precipitation regime can also be expected after large volcanic eruptions; these include, among others, rainfall deficit in monsoon prone regions and in Southern Europe (Joseph and Zeng, 2011) as well as wetter than normal conditions in Northern Europe (Robock and Liu 1994; Gillet et al., 2004; Peng et al., 2009; Meronen et al., 2012; Iles et al., 2013; Wegmann et al., 2014). However, despite recent advances in the field, the impacts of stratospheric volcanic eruptions on the hydro-climatic variability at regional scales remain largely unknown. Therefore, this relevant knowledge about moisture anomalies is critically needed, especially at high-latitude sites where tree growth is mainly limited by summer temperatures.

As dust and aerosol particles of large volcanic eruptions affect primarily the radiation regime, three major drivers of plant growth, i.e. photosynthetic active radiation (PaR), temperature and vapor pressure deficit (VPD) will be affected by volcanic activity. This is reflected in reduced TRW as a result of reduced photosynthesis but even more so by low temperature. As cell division is temperature dependent, its rate (tree-ring growth) will exponentially decrease with decreasing temperature below +3°C (Körner, 2015), outweighing the “low light / low-photosynthesis” effect by far.

Furthermore, over the last years, some studies using mainly carbon isotopic signals ($\delta^{13}C$) in tree rings showed eco-physiological responses of trees to volcanic eruptions at mid- (Battipaglia et al., 2007) or high- (Gennaretti et al., 2017) latitudes. By contrast, a combination of both carbon ($\delta^{13}C$) and oxygen ($\delta^{18}O$) isotopes in tree rings has been employed only rarely to trace CE volcanic eruptions in high-latitude or high-altitude proxy records (Churakova (Sidorova) et al., 2014).

Approaches including TRW, MXD and cell wall thickness (CWT) as well as $\delta^{13}C$ and $\delta^{18}O$ in tree cellulose are a promising way to disentangle hydro-climatic variability as well as winter and early spring temperatures at high-latitude and high-altitude sites (Kirdyanov et al., 2008; Sidorova et al., 2008, 2010, 2011; Churakova (Sidorova) et al., 2014, Castagneri et al., 2017). In that sense, recent work has allowed the retrieval of high-resolution, seasonal information on water and carbon limitations on growth during spring and summer from CWT measurements (Panyushkina et al., 2003; Sidorova et al., 2011; Fonti et al., 2013; Bryukhanova et al., 2015). Depending on site conditions, $\delta^{13}C$ variations reflect light (stand density) (Loader et al., 2013), water availability (soil properties) and air humidity (proximity to open waters, i.e. rivers, lakes, swamps and orography) as these parameters have been recognized to modulate stomatal conductance (g_l) controlling carbon isotopic discrimination.

Depending on the study site, a decrease in the carbon isotope ratio can be expected after stratospheric volcanic eruptions due to limited photosynthetic activity and higher stomatal conductance, which in turn would be the result of decreased temperatures, VPD and a reduction in light intensity. By contrast, volcanic eruptions have also been credited for an increase in photosynthesis as dust and aerosol particles cause an increased light scattering, compensating for the light reduction (Gu et al., 2003). A significant increase in $\delta^{13}C$ values in tree-ring cellulose should be interpreted as an indicator of drought (stomatal closure) or high photosynthesis (Farquhar et al., 1982).

In the past, very limited attention has been given to the elemental and isotopic composition of tree rings in years during which they may have been subjected to the climatic influence of powerful, but remote, and often tropical, volcanic eruptions.

In this study, we aim to fill this gap by investigating the response of different components of the Siberian climate system (i.e. temperature, precipitations, VPD, and sunshine duration) to stratospheric volcanic events of the last 1,500 years. By doing so, we seek to extend our understanding of the effects of volcanic eruptions on climate by combining multiple climate sensitive variables measured in tree rings that were formed around the time of the major volcanic eruptions (see Table 1). We focus our investigation on remote sites in Siberia, two at high latitude (northeastern Yakutia YAK and eastern Taimyr TAY) and one at high altitude (Russian Altai, ALT), where long tree-ring chronologies with high climate sensitivity exist. We developed a dataset including five tree-ring proxies: TRW, MXD, CWT, $\delta^{13}C$ and $\delta^{18}O$ stable isotope chronologies derived from larch trees with the goal: (1) to determine the major climatic drivers of the above mentioned proxies and to evaluate their suitability in terms of climate responsiveness, for each proxy separately and in combination; and based on these analyses (2) to reconstruct the climatic effect of the strong volcanic eruptions over specific periods of the past (Table 1).

2. Material and methods

2.1. Study sites

The study sites are situated in Siberia (Russian Federation), far away from industrial centers (and 1500 – 3400 km apart from each other), in zones characterized by continuous permafrost in northeastern Yakutia (YAK, 69°N, 148°E), eastern Taimyr (TAY, 70°N, 103°E) and in the Altai mountains (ALT, 50°N, 89°E) (Fig. 1a, Table 2). Tree-ring samples were collected during several expeditions and included old relict wood and living larch trees, *Larix cajanderi* Mayr (max. 1216 years) in YAK, *Larix gmelinii* Rupr. (max. 640 years) in TAY and *Larix sibirica* Ldb. (max. 950 years) in ALT. TRW chronologies have been developed and published in the past (Fig. 1, Hughes et al., 1999; Sidorova and Naurzbaev 2002; Sidorova 2003 for YAK; Naurzbaev et al., 2002 for TAY; Myglan et al., 2008 for ALT).

Due to the remote localization of our study sites, we used meteorological data from monitored weather stations located at distances ranging from 50-200 km from the sampling sites. Temperature data from these weather stations are significantly correlated ($r>0.91$; $p<0.05$) with gridded data (http://climexp.knmi.nl). However, poor correlation is found with precipitation data ($r<0.45$; $p<0.05$), most likely as a result representing local effects (Churakova (Sidorova) et al., 2016).

Mean annual air temperature is lower at the high-latitude YAK and TAY sites than at the high-altitude ALT site (Table 2). Annual precipitation totals are very low for all study sites. The vegetation period calculated with a growth threshold of +5°C (Fritts 1976; Schweingruber 1996) is very short (50-120 days) at all locations (Table 2). Sunshine duration for tree growth is higher at YAK and TAY (ca. 18-20 h/day in summer) compared to ALT (ca. 18 h/day in summer) (Sidorova et al., 2005; Myglan et al., 2008; Sidorova et al., 2011; Churakova (Sidorova) et al., 2014).

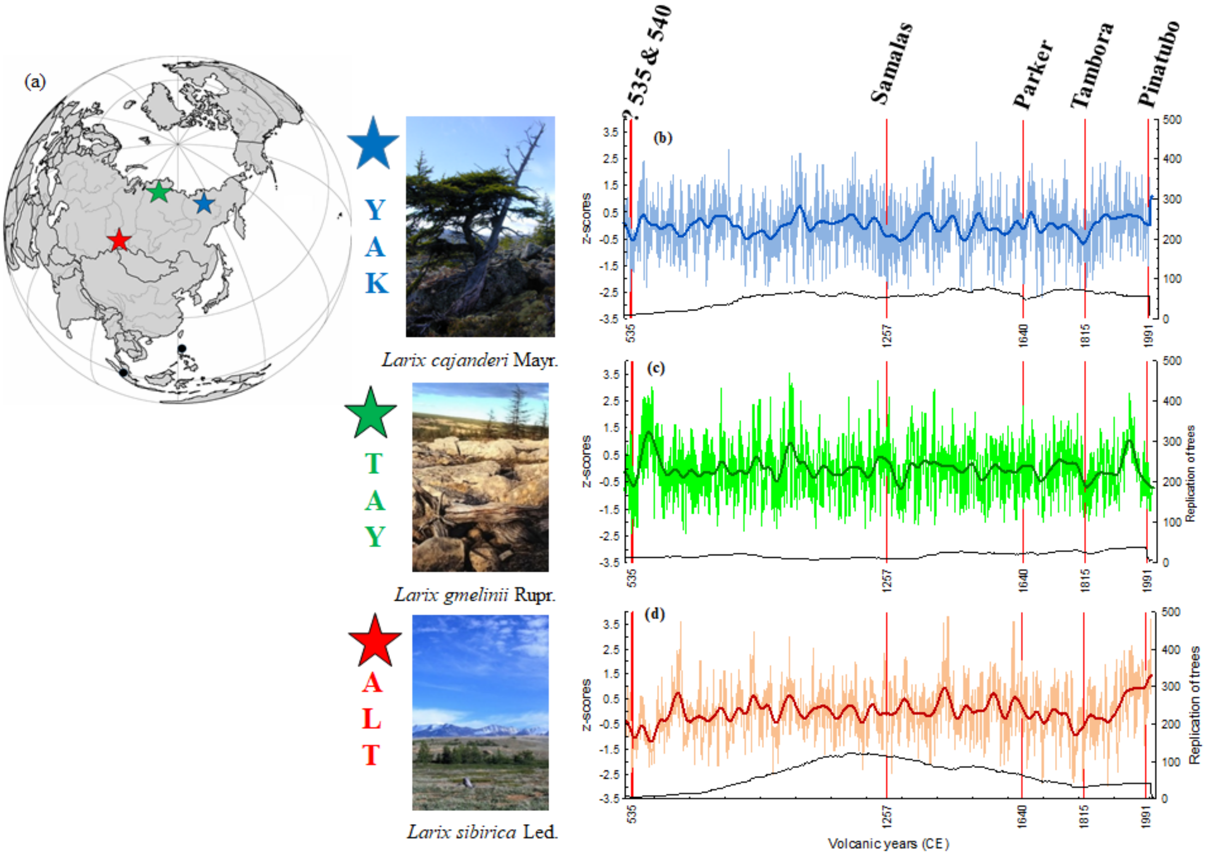

Fig. 1. Map with the locations of the study sites (stars) and volcanic eruptions from the tropics (black dots) considered in this study (a). Annual tree-ring width index (light lines) and smoothed by 51-year Hamming window (bold lines) chronologies from northeastern Yakutia (YAK - **blue**, b) (Hughes et al., 1999; Sidorova and Naurzbaev 2002; Sidorova 2003), eastern Taimyr (TAY - **green**, c) (Naurzbaev et al., 2002), and Russian Altai (ALT - **red**, d) (Myglan et al., 2009) were constructed based on larch trees (Photos: V. Myglan – ALT, M. M. Naurzbaev – YAK, TAY).

2.2. Selection of volcanic events and larch subsamples

Identification of the events analyzed in this study was based on volcanic aerosols deposited in ice core records (Zielinski 1994; Robock 2000), and more precisely on Toohey and Sigl (2017) where the authors listed the top 20 eruptions from the past 2000 years in terms of volcanic stratospheric sulfur injection (VSSI) in a new ice core-based volcanic forcing reconstruction.

Our sub-criteria is based on literature review of reconstructed VSSI and events well reported in tree-ring proxies that may have had a noticeable impact on the forest ecosystems from high-latitude and high-altitude regions (Briffa et al., 1998; D'Arrigo et al., 2001; Churakova (Sidorova) et al., 2016; Büntgen et al., 2016; Gennaretti et al., 2017; Helama et al., 2018). Therefore, based on our previously published TRW and newly developed MXD, CWT, $\delta^{13}C$ and $\delta^{18}O$ in tree-ring cellulose chronologies, we selected the years, characterized by strong volcanic eruptions with far-reaching climatic effect, namely the years CE 535, 540, 1257, 1640, 1815, and 1991. Therefore, to investigate climatic impacts of these eruptions in Siberian regions, we selected periods around (± 10 years): CE 525-545, 1247-1267, 1630-1650, 1805-1825, and 1950-2000, with the latter being used to calibrate tree-ring proxy versus available climate data (Table 2).

Material was prepared from the 2000-yr long TRW chronologies available at each of the sites from the previous studies (Fig. 1 b-d). According to the level of conservation of the material, the largest possible number of samples was prepared for each of the proxies. Unlike TRW, which could be measured on virtually all samples, some of the material was not available with sufficient quality to allow for tree-ring anatomy and stable isotope analysis. We therefore use a smaller sample size for CWT (n=4) and stable isotopes (n=4) than for TRW (n=12) or MXD (n=12). Nonetheless, replications are still comparable with those used in reference papers in the fields of CWT and isotope analyses (Loader et al., 1997; Panyushkina et al., 2003).

Table 1. List of stratospheric volcanic eruptions used in the study.

Study period (CE)	Date of eruption Month/Day/Year	Volcano name	Volcanic Explosivity Index (VEI)	Location, coordinates	References
525-545	NA/NA/535	Unknown	?	Unknown	Stothers, 1984
	NA/NA/540	Unknown	?	Unknown	Sigl et al., 2015; Toohey, Sigl 2017
1247-1267	May-October/NA/ 1257	Samalas	7	Indonesia, 8.42°N, 116.47°E	Lavigne et al., 2013; Stothers, 2000; Sigl et al., 2015
1630-1650	December/26/1640	Parker	5	Philippines, 6°N, 124°E	Zielinski et al., 1994
1805-1825	April/10/1815	Tambora	7	Indonesia, 8°S, 118°E	Zielinski et al., 1994
1950 - 2000	June/15/1991	Pinatubo	6	Philippines, 15°N, 120°E	Zielinski et al., 1994; Sigl et al., 2015

NA – not available.

Table 2. Summary of tree-ring sites in northeastern Yakutia (YAK), eastern Taimyr (TAY), and Altai (ALT) and weather stations used in the study. Monthly air temperature (T, °C), precipitation (P, mm), sunshine duration (S, h/month) and vapor pressure deficit (VPD, kPa) data were used from the available meteorological database: http://aisori.meteo.ru/ClimateR.

Site	Species	Location	Weather station	Meteorological parameters T (°C)	P (mm)	S (h/month)	VPD (kPa)	Length of vegetation period (day)	Thawing permafrost depth (max, cm)	Annual air temperature (°C)	Annual precipitation (mm)
				Periods							
YAK	*Larix cajanderi* Mayr.	69°N, 148°E	Chokurdach 62°N, 147°E, 61 m. a.s.l.	1950-2000	1966-2000	1961-2000	1950-2000	50-70*	20-50*	-14.7	205
TAY	*Larix gmelinii* Rupr.	70°N, 103°E	Khatanga 71°N, 102°E, 33m. a.s.l.	1950-2000	1966-2000	1961-2000	1950-2000	90**	40-60**	-13.2	269
ALT	*Larix sibirica* Ledeb.	50°N, 89°E	Mugur Aksy 50°N, 90°E 1850 m. a.s.l.	1963-2000	1966-2000			90-120***	80-100***	-2.7	153
			Kosh-Agach 50°N, 88°E 1758 m.a.s.l.			1961-2000	1950-2000				

*Abaimov, 1996; Hughes et al., 1999; Churakova (Sidorova) et al., 2016

**Naurzbaev et al., 2002

***Sidorova et al., 2011

2.3. Tree-ring width analysis

Ring width of 12 trees was re-measured for each selected period. Cross-dating was checked by comparison with the existing complete 2000-yr TRW chronologies (Fig. 1). The TRW series were standardized using the ARSTAN program (Cook and Krusic, 2008) based on the negative exponential curve (k>0) or a linear regression (any slope) prior to bi-weight robust averaging (Cook and Kairiukstis 1990). Signal strength in regional TRW chronologies was assessed with the Expressed Population Signal (EPS) statistics as it measures how well the finite sample chronology compares with a theoretical population chronology based on an infinite number of trees (Wigley et al., 1984). Mean inter-series correlation (RBAR) and EPS values of stable isotope chronologies were calculated for the period 1950-2000, for which individual trees were analyzed separately. We show the common signal with an EPS > 0.85 and series have RBAR ranging between 0.59 and 0.87. Before 1950, we used pooled material only. For all other tree-ring parameters, the EPS exceeds the threshold of 0.85, and RBAR values range from 0.63 to 0.94.

2.4. Image analysis of cell wall thickness (CWT)

Analysis of wood anatomical features was performed for all studied periods with an AxioVision scanner (Carl Zeiss, Germany). Micro-sections were prepared using a sliding microtome and stained with methyl blue (Furst, 1979). Tracheids in each tree ring were measured along five radial files of cells (Munro et al., 1996; Vaganov et al., 2006) selected for their larger tangential cell diameter (T). For each tracheid, CWT was computed separately. In a second step, tracheid anatomical parameters were averaged for every tree ring. Site chronologies are presented for the complete annual ring chronology without standardization due to the absence of low-frequency trend. CWT data from ALT for the periods 1790-1835 and 1950-2000 were used from the past studies (Sidorova et al., 2011; Fonti et al., 2013) and for YAK for the period from 1600-1980 from Panyushkina et al. (2003). Unfortunately the remaining sample material for the CE 536 ring at TAY was insufficient to produce a clear anatomical signal. As a result, CWT is missing for CE 536 at TAY (Fig. 2).

2.5. Maximum latewood density (MXD)

Maximum latewood density chronologies from ALT were available continuously for the period CE 1407-2007 from Schneider et al. (2015) and for YAK and TAY the period CE 1790-2004 from Sidorova et al. (2010). For any of the other periods, at least six cross-sections (for CE 516-560, only four sections could be used, as this period is not as well replicated) were sawn with a double-bladed saw, to a thickness of 1.2 mm, at right angles to the fiber direction. Samples were exposed to X-rays for 35-60 min (Schweingruber 1996). MXD measurements were obtained with a resolution of 0.01 mm, and brightness variations transferred into (g/cm^3) using a calibration wedge (Lenz et al., 1976; Eschbach et al., 1995) from a Walesch X-ray densitometer 2003. All MXD series were detrended in ARSTAN by calculating subtractions from straight-line functions (Fritts, 1976). Site chronologies were developed for each volcanic period using the bi-weight robust averaging.

2.6. Stable carbon ($\delta^{13}C$) and oxygen ($\delta^{18}O$) isotopes in tree-ring cellulose

During photosynthetic CO_2 assimilation $^{13}CO_2$ is discriminated against $^{12}CO_2$, leaving the newly produced assimilates depleted in ^{13}C. The carbon isotope discrimination ($^{13}\Delta$) is partitioned in the diffusional component with a = 4.4‰ and the biochemical fractionation with b = 27‰, for C3 plants, during carboxylation via Rubisco. The $^{13}\Delta$ is directly proportional to the c_i/c_a ratio, where c_i is the leaf intercellular, and c_a the ambient CO_2 concentration. This ratio reflects the balance between stomatal conductance (g_l) and photosynthetic rate (A_N). A decrease in g_l at a given A_N results in a decrease of $^{13}\Delta$, as c_i/c_a decreases and vice versa. The same is true when A_N increases or decreases at a given g_l. Since CO_2 and H_2O gas exchange are strongly interlinked with the C-isotope fractionation $^{13}\Delta$ is controlled by the same environmental variables i.e. PaR, CO_2, VPD and temperature (Farquhar et al., 1982, 1989; Cernusak et al., 2013).

The oxygen isotopic compositions of tree-ring cellulose record the $\delta^{18}O$ of the source water derived from precipitation, which itself is related to temperature variations at middle and high latitudes (Craig, 1961; Daansgard, 1964). It is modulated by evaporation at the soil surface and to a larger degree by evaporative and diffusion processes in leaves; the process is largely controlled by the vapor pressure deficit (Dongmann et al., 1972, Farquhar and Loyd, 1993, Cernusak et al., 2016). A further step of fractionation occurs as sugar molecules are transferred to the locations of growth (Roden et al., 2000). During the formation of organic compounds the biosynthetic fractionation leads to a positive shift of the $\delta^{18}O$ values by 27‰ relative to the leaf water (Sternberg, 2009). The oxygen isotope variation in tree-ring cellulose therefore reflects a mixed climate information, often dominated by a temperature, source water or sunshine duration modulated by the VPD influence.

The cross-sections of relict wood and cores from living trees used for the TRW, MXD and CWT measurements were then selected for the isotope analyses. We analyzed four subsamples for each studied period according to the standards and criteria described in Loader et al. (2013). The first 50 yrs. of each sample were excluded to limit juvenile effects (McCarroll and Loader, 2004). After splitting annual rings with a scalpel, the whole wood samples were enclosed in filter bags. α-cellulose extraction was performed according to the method described by Boettger et al. (2007). For the analyses of $^{13}C/^{12}C$ and $^{18}O/^{16}O$ isotope ratios, 0.2-0.3 mg and 0.5-0.6 mg of cellulose were weighed for each annual ring, into tin and silver capsules, respectively. Carbon and oxygen isotopic ratios in cellulose were determined with an isotope ratio mass spectrometer (Delta-S, Finnigan MAT, Bremen, Germany) linked to two elemental analyzers (EA-1108, and EA-1110 Carlo Erba, Italy) via a variable open split interface (CONFLO-II, Finnigan MAT, Bremen, Germany). The $^{13}C/^{12}C$ ratio was determined separately by combustion under oxygen excess at a reactor temperature of 1020°C. Samples for $^{18}O/^{16}O$ ratio measurements were pyrolyzed to CO at 1080°C

(Saurer et al., 1998). The instrument was operated in the continuous flow mode for both, the C and O isotopes. The isotopic values were expressed in the delta notation multiplied by 1000 relative to the international standards (Eq. 1):

$$\delta \text{ sample} = R_{sample}/R_{standard}-1 \qquad \text{(Eq. 1)}$$

where R_{sample} is the molar fraction of $^{13}C/^{12}C$ or $^{18}O/^{16}O$ ratio of the sample and $R_{standard}$ the molar fraction of the standards, Vienna Pee Dee Belemnite (VPDB) for carbon and Vienna Standard Mean Ocean Water (VSMOW) for oxygen. The precision is $\sigma \pm 0.1‰$ for carbon and $\sigma \pm 0.2‰$ for oxygen. To remove the atmospheric $\delta^{13}C$ trend after CE 1800 from the carbon isotope values in tree rings (i.e. Suess effect, due to fossil fuel combustion) we used atmospheric $\delta^{13}C$ data from Francey et al. (1999), http://www.cmdl.noaa.gov./info/ftpdata.html). These corrected series were used for all statistical analyses. The $\delta^{18}O$ cellulose series were not detrended.

2.7. Climatic data

Meteorological series were obtained from local weather stations close to the study sites and used for the computation of correlation functions between tree-ring proxies and monthly climatic parameters (Table 2). Sunshine duration data were obtained from available Kosh-Agach meteorological station (http://aisori.meteo.ru/ClimateR).

2.8. Statistical analysis

All chronologies for each period were normalized to z-scores (Fig. 2). To assess post-volcanic climate variability, we used Superposed Epoch Analysis (SEA, Panofsky and Brier, 1958) with the five proxy chronologies available at each of the three study sites. In this experiment, the 10 years before and after a volcanic eruption were analyzed. SEA is applied to the six annually dated volcanic eruptions (Table 1).

To test the sensitivity of the studied tree-ring parameters to climate, bootstrap correlation functions have been computed between proxy chronologies and monthly climate predictors using the 'bootRes' package of R software (R Core Team 2016) for the period 1950 (1966)-2000.

To estimate whether volcanic years can be considered as extreme, we computed Probability Density Functions (PDFs, Stirzaker, 2003) for each study site and for each tree-ring parameter over a period of 221 years for which measurements are available (Fig. S1). A year is considered (very) extreme if the value of a given parameter is below the (5^{th}) 10^{th} percentile of the PDF. We applied unpaired t-test statistics to check significance between each proxy and each site.

3. Results

3.1. Anomalies in tree-ring proxy chronologies after stratospheric volcanic eruptions

Normalized TRW chronologies show negative deviations the year following the eruptions at all studied sites (Fig. 2). Regarding CWT, a strong decrease is observed in CE 536 at YAK and ALT. Only two layers of cells were formed in CE 536 for YAK as compared to the 11-20 layers of cells formed on average during "normal" years. In addition, we also observe the formation of frost rings in ALT between CE 536 and 538, as well as in 1259.

Furthermore, we revealed decreasing MXD values for ALT (-4.4 σ) in CE 537 and YAK (-2.8 σ) in CE 536. However, for TAY, we found less pronounced patterns of the MXD variation (Fig. 2). In this regard, the sharpest decrease was observed in the CWT chronologies from YAK (-2.4σ) in CE 540 compared to a smaller response in TAY and ALT (Fig. 2). The ALT $\delta^{18}O$ chronology recorded a drastic decrease in 536 CE with (- 4.8 σ) (Fig. 2, Fig. S1). A $\delta^{18}O$ decrease for YAK was found after the CE 1257 Samalas eruption, but only in CE 1259, opposite to increased $\delta^{18}O$ values towards CE 1259 from ALT (Fig. 2).

Regarding the carbon isotope ratio, negative anomalies are observed in YAK and TAY, and – to a lesser extent – in ALT. The CE 540 eruption was less clearly recorded in tree-ring proxies from TAY, compared to YAK and ALT (Fig. 2). With respect to the CE 1257 Samalas eruption (Fig.

2), the year following the eruption was recorded as very extreme in the TRW, MXD, $\delta^{18}O$, while less extreme in CWT and $\delta^{13}C$ from YAK. ALT chronologies show a synchronous decrease for all proxies following two years after the eruption (see Fig. S1).

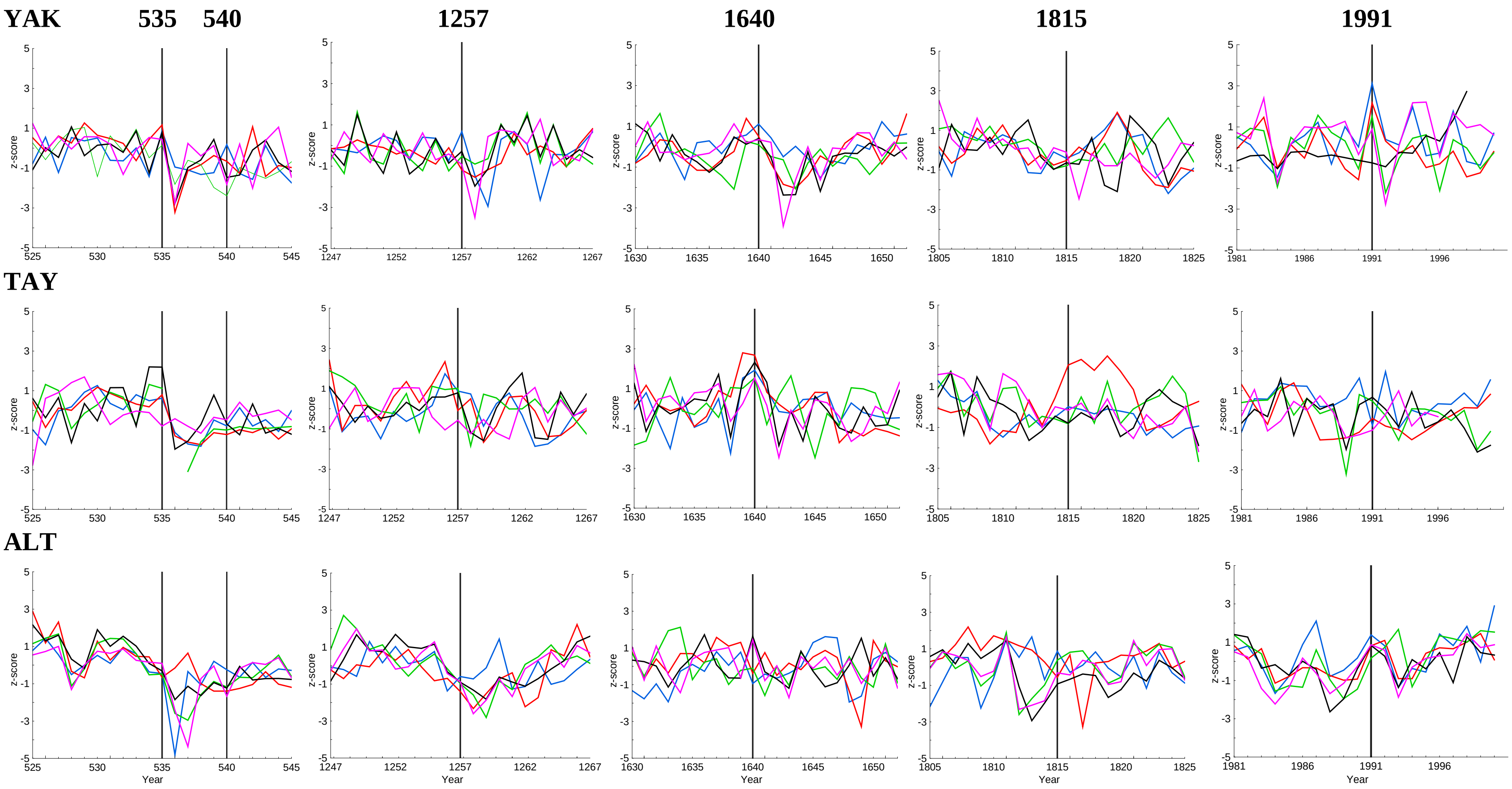

Fig. 2. Normalized (z-score) individual tree-ring index chronologies (TRWi, **black**), maximum latewood density (MXD, **purple**), cell wall thickness (CWT, **green**), $\delta^{13}C$ (**red**) and $\delta^{18}O$ (**blue**) in tree-ring cellulose chronologies from YAK, TAY and ALT for the specific periods 10 years before and after the eruptions CE 535, 1257, 1640, 1815 and 1991 are presented. Vertical lines showed year of the eruptions.

The impacts of the more recent CE 1640 Parker, 1815 Tambora, and 1991 Pinatubo eruptions are, by contrast, far less obvious. In CE 1642, decreasing values are observed in all tree-ring proxies from the high-latitude sites YAK and TAY, whereas tree-ring proxies are not clearly affected at ALT (mainly for the TRW and MXD, less for $\delta^{13}C$ and $\delta^{18}O$).

Hardly any strong anomalies are observed in CE 1816 in Siberia regardless of the site and the tree-ring parameter analyzed. The ALT $\delta^{13}C$ in CE 1817 and YAK MXD in 1816 can be seen as an exception to the rule here as they evidenced extreme values, respectively.

Finally, the Pinatubo eruption is captured in CE 1992 mainly by MXD and CWT chronologies from YAK. Simultaneous decreases of all tree-ring proxies from ALT are observed in 1993 (Fig. 2, S1), which, however, cannot be classified as extreme.

Overall, the SEA (Fig. 3) shows the high spatiotemporal variability and complexity of the response of the Siberian climate system to the largest volcanic events over past millennium (CE 535, 540, 1257, 1640, 1815 and 1991). A short-term response by two years after the eruptions is observed in the CWT proxies for TAY, while for YAK and ALT, the CWT decrease lasts longer (up to 5-6 years in ALT and YAK, respectively) (Fig. 3). The behavior of isotope chronologies is rather more complex, with a distinct decrease in $\delta^{13}C$ at the high-latitude sites (YAK, TAY), whereas $\delta^{18}O$ series are impacted mainly at the high-latitude YAK and high-altitude ALT sites. We find significant differences ($p=0.014$, $df=40$, $n=21$) between averaged $\delta^{13}C$ chronologies of the YAK and ALT sites. SEA for TRW and MXD show a more drastic decrease of values during the first year, mainly for TRW from YAK, and MXD from ALT when compared to other proxies and study sites (Fig. 3).

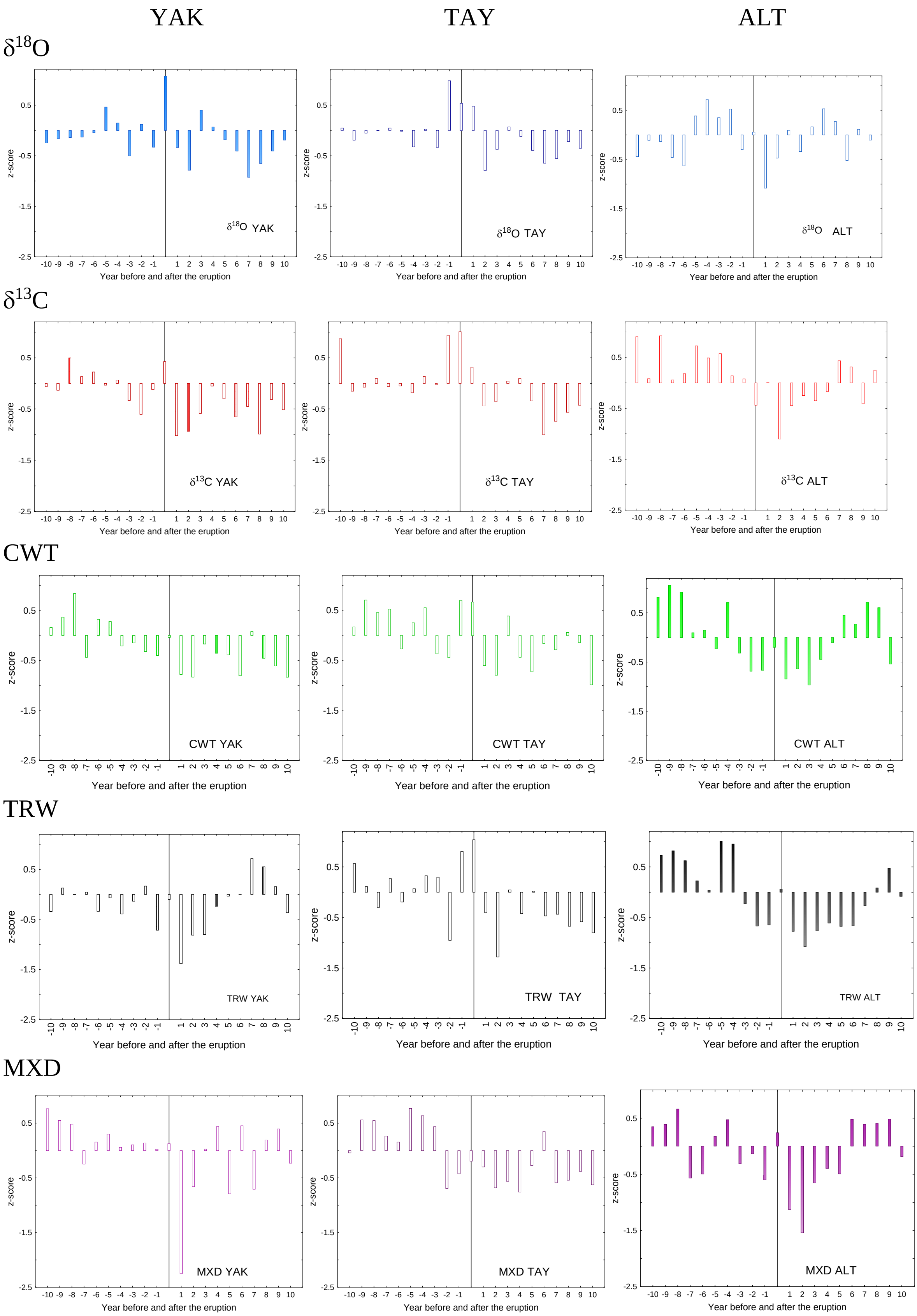
YAK
TAY
ALT
δ18O
δ13C
CWT
TRW
MXD
z-score
Year before and after the eruption
δ18O YAK
δ18O TAY
δ18O ALT
δ13C YAK
δ13C TAY
δ13C ALT
CWT YAK
CWT TAY
CWT ALT
TRW YAK
TRW TAY
TRW ALT
MXD YAK
MXD TAY
MXD ALT

Fig. 3. Superposed epoch analysis of $\delta^{18}O$, $\delta^{13}C$, CWT, TRW and MXD chronologies for the Yakutia (YAK), Taimyr (TAY), and Altai (ALT) sites, summarizing anomalies of the volcanic eruptions in CE 535, 540, 1257, 1640, 1815, and 1991.

3.2. Tree-ring proxies versus meteorological series

3.2.1. Monthly air temperatures and sunshine duration

Bootstrapped functions established for the instrumental period evidence significant positive correlations ($p<0.05$) between TRW and MXD chronologies and mean summer (June-July) temperatures at all sites. Temperatures at the beginning (June) and the end of the growing season (mid-August) influenced the MXD chronology in ALT (r = 0.57) and YAK (r = 0.55), respectively (Fig. 4). July temperatures appear as a key factor for determining tree growth as they significantly impact CWT, $\delta^{13}C$, and $\delta^{18}O$ (with the exception of TAY for the latter) chronologies (r=0.28-0.60) at YAK and ALT.

Correlation analysis between July temperature and July sunshine duration showed significant correlation for YAK (r=0.56) and ALT (r=0.34). July sunshine duration are strongly and positively correlated with $\delta^{18}O$ in larch tree-ring cellulose chronologies from YAK (r=0.73) and ALT (r=0.51) for the period 1961-2000.

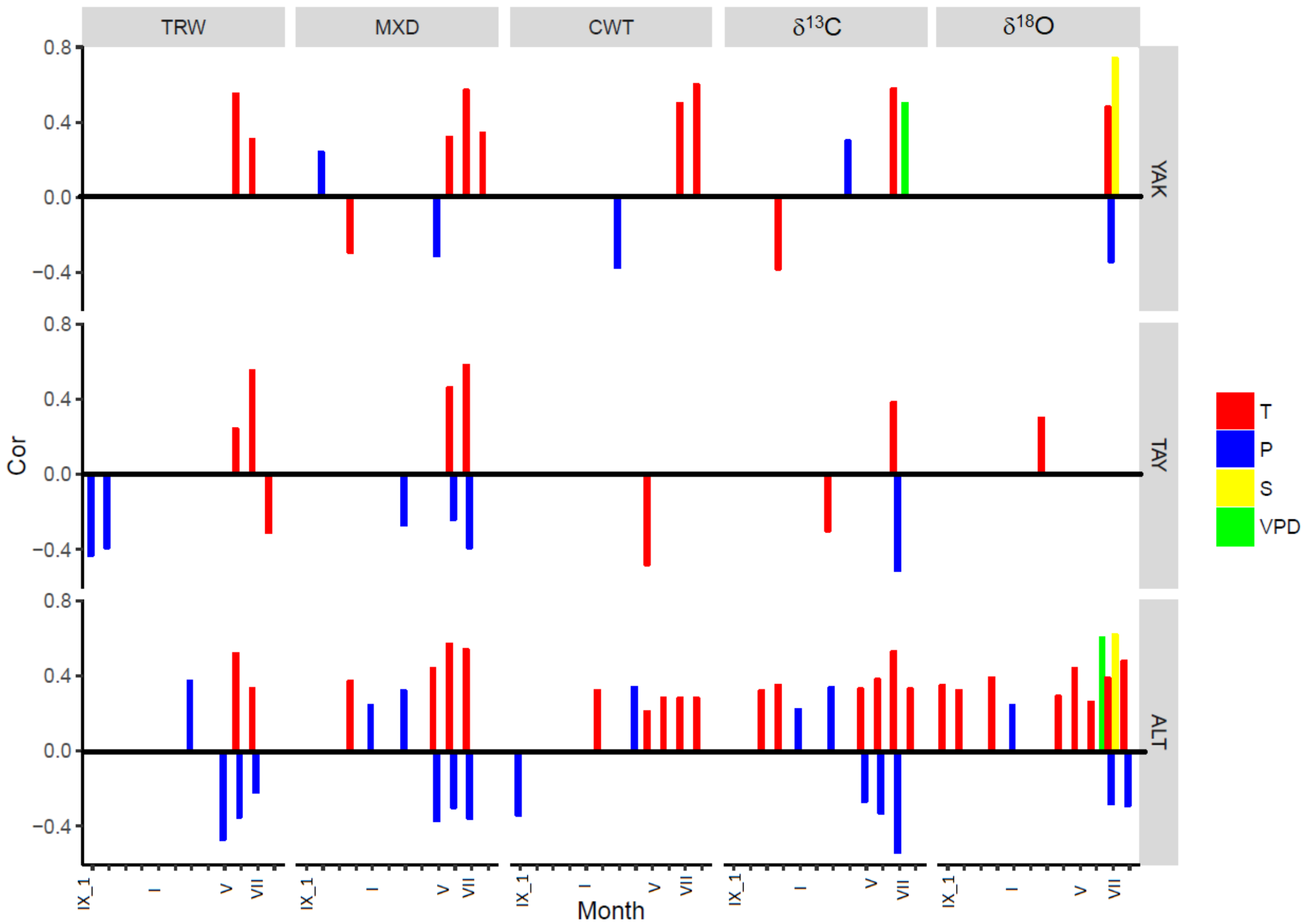

Fig. 4. Significant correlation coefficients between tree-ring parameters: TRW, MXD, CWT, $\delta^{13}C$ and $\delta^{18}O$ versus weather station data: temperature (T, red), precipitation (P, blue), vapor pressure deficit (VPD, green), and sunshine duration (S, yellow) from September of the previous year to August of the current year for three study sites were calculated. Table 2 lists stations used in the analysis.

3.2.2. Monthly precipitation

The strongest July precipitation signal is observed at ALT (r=-0.54) and TAY (r=-0.51) with $\delta^{13}C$ chronologies ($p<0.05$). In addition, at ALT a positive relationship is observed between March precipitation and TRW ($p<0.05$) (r=0.37), MXD (r=0.32), while April precipitation is related positively with CWT (r=0.34), respectively. At YAK, July precipitation showed negative relationship with $\delta^{18}O$ in tree-ring cellulose (r=-0.34; $p<0.05$) only.

3.2.3. Vapor pressure deficit (VPD)

June VPD is significantly and positively correlated with the $\delta^{18}O$ chronology from ALT (r=0.67 *p<0.05*, respectively) for the period 1950-2000. The $\delta^{13}C$ in tree-ring cellulose from YAK correlate with July VPD only (r=0.69 *p<0.05*). We did not find a significant influence of VPD in TAY tree-ring and stable isotope parameters.

3.2.4. Synthesis of the climate data analysis

In summary, we found that during the instrumental period of weather station observations (Table 2) mainly summer temperature influenced TRW, MXD and CWT for the high-latitude sites (YAK, TAY), while stable carbon and oxygen isotopes were affected by summer precipitation (YAK, TAY, ALT), sunshine duration (YAK, ALT), and vapor pressure deficit (YAK, ALT) signals.

3.3. Response of Siberian larch trees to climatic changes after the major volcanic eruptions

Based on the statistical analysis above for the calibration period, we assumed that these relationships would not change over time and will provide information about climatic changes during past volcanic periods (Fig. 5).

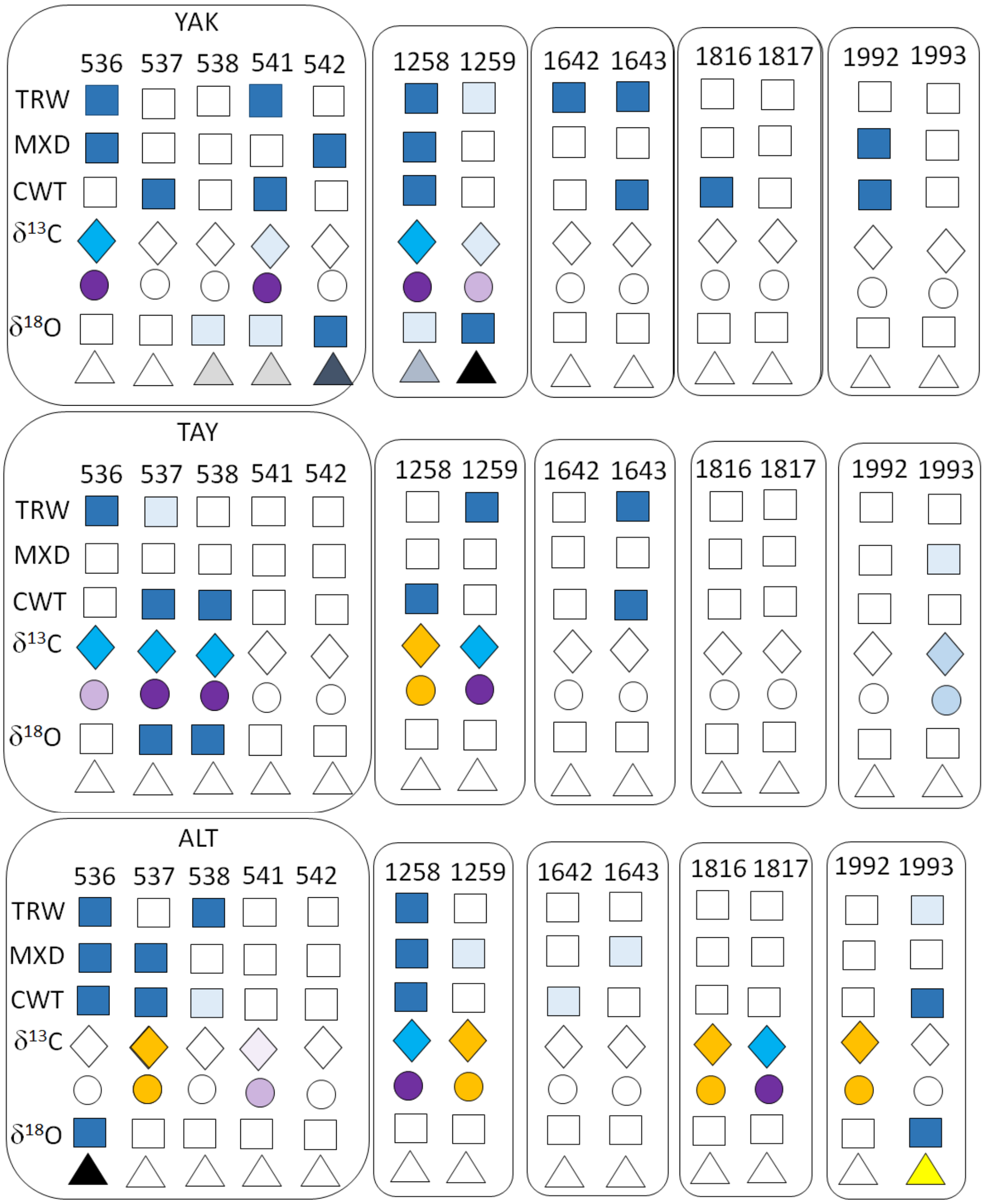

Fig. 5. Response of larch trees from Siberia to the CE volcanic eruptions (Table 1) with percentile of distribution considered as very extreme (< 5th, intensive color), extreme (>5th, <10th, light color) and non-extreme (>10th, white color). July temperature changes presented as a square from **heavy blue** (cold) to **light blue** (moderate). Summer vapor pressure deficit (VPD) variabilities are shown as a circle from **purple** (low), light purple (moderate decrease) to **orange** (increase, developing to dry air). July precipitation presented as a rhomb from **heavy turquoise** (wet), **light blue** (moderate) to **orange** (dry). Low July sunshine duration shown as black triangle, while high – as yellow.

3.3.1. Temperature proxies

We found strong negative summer air temperature anomalies at all sites after the CE 535 and 1257 volcanic eruptions. The temperature decrease was found in the TRW and CWT datasets at all sites, and also in the MXD datasets at YAK and ALT (Fig. 5). For the volcanic eruptions in later centuries, the evidence for a decrease in temperature was not as pronounced. Namely, no strong drop in summer temperature was found for ALT in CE 1642 nor 1643, an extreme cold in TAY for 1643 only, while still a cold summer in YAK for these two years based on the TRW chronology; 1816 was cold only in YAK (based on the CWT chronology), but not at the other sites. CE 1992 was recorded as a cold year in MXD and CWT from YAK, but again not for the other sites; CE 1993 was an extremely cold year for ALT based on CWT and $\delta^{18}O$, while also sunny, which is confirmed by local weather station data.

3.3.2. Moisture proxies: precipitation and VPD

Based on the climatological analysis with the local weather stations data (Table 2, Fig. 4) for all studied sites we considered $\delta^{13}C$ in tree-ring cellulose chronologies as proxies for precipitation and vapor pressure deficit (VPD) changes. Yet, CWT from ALT could be considered as a proxy with mixed temperature and precipitation signal (Fig. 4, Fig. 5). Accordingly, the $\delta^{13}C$ values showed humid summer climate conditions for YAK in 536, 541; for TAY in 536, 537, 538 and in the year of 541 for ALT. Opposite to other proxies and sites, the year of CE 537 in ALT was rather dry (Fig. 5). Dry conditions prevailed in CE 1258 in TAY, in CE 1259 in ALT, whereas wet anomalies were recorded in 1258 and 1259 in YAK. No anomalies were recorded for the CE 1642 event, irrespective of the sites. A rather wet summer was reconstructed for ALT in CE 1817 compared to 1816. CE 1992 in ALT was dry, which is consistent with weather station data (Fig. 5). Overall, there were mostly wet or humid anomalies at the high-latitude sites after the eruptions, but the response greatly varied between the different events.

3.3.3. Sunshine duration proxies

Instrumental measurements of sunshine duration (Table 2) in YAK and ALT during the recent period showed a significant link with $\delta^{18}O$ cellulose. Based on this we conclude that sunshine duration decreased significantly after various eruptions in YAK (538, 541, 542, 1258 and 1259) and in 536 in ALT. Conversely, summer 1993 in ALT was very sunny (Fig. 5).

4. Discussion

In this paper, we analyze climatic anomalies in years following selected, large volcanic eruptions of the CE using long-term, tree-ring multi-proxy chronologies for $\delta^{13}C$ and $\delta^{18}O$, TRW, MXD, CWT for the high-latitude (YAK, TAY) and high-altitude (ALT) sites. Since trees as living organisms respond to various climatic impacts, the carbon assimilation and growth patterns accordingly leave unique "finger prints" in the photosynthates, which is recorded in the wood of the tree rings specifically and individually for each proxy.

4.1. Evaluation of the applied proxies in Siberian tree-ring data

This study clearly shows that each proxy has to be analyzed and interpreted specifically for its validity on each studied site and evaluated for its suitability for the reconstruction of abrupt climatic changes.

TRW in temperature-limited environments is an indirect proxy for summer temperature reconstructions, as growth is a temperature-controlled process. Temperature clearly determines the duration of the growing season and the rate of cell division (Cuny et al., 2014). Accordingly, low growing season temperatures are reflected in narrow tree rings. The upper temperature limit is species and biome specific. In most cases tree growth is limited by drought rather than by high temperatures, since water shortage and VPD increase with increasing temperature. Still this does not make TRW a suitable proxy to determine the influence of water availability and air humidity, especially at the temperature-limited sites.

MXD chronologies obtained for the Eurasian subarctic record mainly a July-August temperature signal (Vaganov et al., 1999; Sidorova et al., 2010; Büntgen et al., 2016) and add valuable information about climate conditions toward the end of the growth season. Similarly, CWT is an anatomical parameter, which contains information on carbon sink limitation of the cambium due to extreme cold conditions (Panyushkina et al., 2003; Fonti et al., 2013; Bryukhanova et al., 2015). The clear signal about reduced number of cells within a season, for example, strong decreasing CWT in CE 536 at YAK or formation of frost rings in ALT (CE 536-538, 1259) has been shown in our study.

Low $\delta^{13}C$ values can be explained by a reduction in photosynthesis caused by volcanic dust veils. For the distinction whether $\delta^{13}C$ is predominantly determined by A_N or g_l the combined evaluation with $\delta^{18}O$ or TRW is needed. High $\delta^{18}O$ values indicate high VPD, which induces a reduction in stomatal conductance, reducing the back diffusion of depleted water molecules from the ambient air. This confirms a sunny year CE 1993 in ALT with warm and dry weather conditions. Interestingly, we also find less negative values for $\delta^{13}C$ in the same period. This shows that the two isotopes correlate with each other and indicates the need for a combined evaluation of the C and O isotopes (Scheidegger et al., 2000) taking into account precautions as suggested by Roden and Siegwolf (2012).

4.2. Lag between volcanic events and response in tree rings

In most of the discussed events, we observe a certain delay – or lag – between the eruption and the response in tree rings of one year or more (Fig. 3). This lag is explained by the tree's use of stored carbohydrates, which are the substrate for needle and early wood production. These stored carbohydrates carry the isotopic signal of previous years and depending on their remobilization and use mask the signals in freshly produced biomass. The delayed signal could also reflect the time needed for the dust veil to be transported to the study sites.

4.3. Temperature and sunshine duration changes after stratospheric volcanic eruptions

Correlation functions show that MXD and CWT (with the exception of TAY in the latter case), and to a lesser extent also TRW chronologies, portray the strongest signals for summer (June-August) temperatures. In addition, significant information about sunshine duration can be derived from the YAK and ALT $\delta^{18}O$ series. Thus, we hypothesize that extremely narrow TRW and very negative anomalies observed in the MXD and CWT chronologies of YAK and to a lesser extent at ALT, in CE 536 and 1258 along with low $\delta^{18}O$ values (except for ALT in CE 1257) reflect cold conditions in summer. Presumably, the temperatures were below the threshold values for growth (Körner, 2015). This hypothesis of a generalized regional cooling after both eruptions is further confirmed by the occurrence of frost rings at ALT site in CE 538, 1259 (Myglan et al., 2008; Guillet et al., 2017), as well as in neighboring Mongolia (D'Arrigo et al., 2001). The unusual cooling in CE 536 is also evidenced by a very small number of cells formed at YAK (Churakova (Sidorova) et al., 2014). Although $\delta^{18}O$ is an indirect proxy for needle temperature, low $\delta^{18}O$ values in CE 536 and 1258 for YAK and ALT are a result of low irradiation, leading to low temperature and low VPD (high stomatal conductance), both likely a result from volcanic dust veils.

Similarly, in the aftermath of the Samalas eruption, the persistence of summer cooling is limited to CE 1259 only at the three study sites, which is in line with findings of Guillet et al., (2017). Interestingly, a slight decrease in oxygen isotope chronologies – which can be related to low levels of summer sunshine duration (i.e. low leaf temperatures) – allows for hypothesizing that cool conditions could have prevailed.

For all later high-magnitude CE eruptions, temperature-sensitive tree-ring proxies do not evidence a generalized drop in summer temperatures. Paradoxically, the impacts of the Tambora eruption, known for its triggering of a widespread "year without summer" (Harrington, 1992), did only induce abnormal MXD at YAK, but no anomalies are observed at sites TAY and ALT, except for the positive deviation of $\delta^{13}C$ in TAY and the negative anomaly in CE 1817 for ALT (Fig. 2). While these findings may seem surprising, they are in line with the TRW and MXD reconstructions of Briffa et al., (1998) or Guillet et al., (2017), who found limited impacts of the CE 1815 Tambora event in Eastern Siberia and Alaska using TRW and MXD data only. The inclusion of CWT chronologies, not used in their reconstructions, further confirm the absence of a significant cooling in this region following the second largest eruption of the last millennium.

Finally, in CE 1992, our results evidence cold conditions in YAK, which is consistent with weather observations showing that the below-average anomalies in summer temperatures (after Pinatubo eruption) were indeed limited to Northeastern Siberia (Robock, 2000). As both isotopes indicate a reduction in stomatal conductance, we found that warm (in agreement with MXD and CWT) and dry conditions were prevalent for ALT at this time. This isotopic constellation was confirmed by the positive relationships between VPD and $\delta^{18}O$ and $\delta^{13}C$ for ALT. However, temperature and sunshine duration are not always highly coherent over time due to the influence of other factors, like Arctic Oscillations as it was suggested for Fennoscandia regions by Loader et al. (2013).

4.4. Moisture changes

Water availability is a key parameter for Siberian trees as they are growing under extremely continental conditions with hot summers and cold winters, and even more so with very low annual precipitation (Table 2). Continuous permafrost, in addition, is playing a crucial role, and can be considered as a buffer for additional water sources during hot summers (Sugimoto et al., 2002; Boike et al., 2013; Saurer et al., 2016). Yet, thawed permafrost water is not always available for roots due to the surficial structure of the root plate or extremely cold water temperature (close to 0ºC), which can hardly be utilized by trees (Churakova (Sidorova) et al., 2016). Thus, Siberian trees are highly susceptible to drought, induced by dry and warm air during July and therefore the stable carbon isotopes can be sensitive indicators of such conditions. After volcanic eruptions, however, low light intensity due to dust veils induce low temperatures and reduced VPD, the driver for evapotranspiration. Under such conditions drought stress is unlikely to occur. However, the transition phases with changes from cool and moist to warm and dry conditions are more critical when drought is more likely to occur.

In our study, higher $\delta^{13}C$ values in tree-ring cellulose indicate increasing drought conditions as a consequence of reduced precipitation for two years after the CE 1257 volcanic eruption at all three sites. No further extreme hydro-climatic anomalies occurred at Siberian sites in the aftermath of the Pinatubo eruption.

4.5. Synthetized interpretation from the multi-parameter tree-ring proxies

Our analysis demonstrates the added value of a tree-ring derived multi-proxy approach to better capture the climatic variability after large volcanic eruptions. Besides the well-documented effects of temperature derived from TRW and MXD, CWT, stable carbon and oxygen isotopes in tree-ring cellulose provide important and complementary information about moisture and sunshine duration changes (an indirect proxy for leaf temperature effective for air-to-leaf VPD) after stratospheric volcanic eruptions.

In detail, our results reveal a complex behavior of the Siberian climatic system to the stratospheric volcanic eruptions of the Common Era. The CE 535 and CE 1257 Samalas eruptions caused substantial cooling – very likely induced by dust veils (Churakova (Sidorova) et al., 2014; Guillet et al., 2017; Helama et al., 2018) – as well as humid conditions at the high-latitude sites. Conversely, only local climate responses were observed after the CE 1641 Parker, 1815 Tambora, and 1991 Pinatubo eruptions. Similar site-dependent impacts were found in CE 1453, 1458 and 1601 (Fig. S1), frequently referred to as the coldest summers of the last millennium in the Northern Hemisphere based on TRW and MXD reconstructions (Schneider et al., 2015; Stoffel et al., 2015; Wilson et al., 2016; Guillet et al., 2017). This absence of widespread and intense cooling or reduction of precipitation over vast regions of Siberia may result from the location and strength of the volcanic eruption, atmospheric transmissivity as well as from the modulation of radiative forcing effects by regional climate variability. These results are consistent with other regional studies, which interpreted the spatio-temporal heterogeneity of tree responses to past volcanic events (Wiles et al., 2014; Esper et al., 2017; Barinov et al., 2018) in terms of regional climate peculiarities.

5. Conclusions

In this study, we demonstrate that the consequences of volcanic eruptions on climate are rather complex between sites and among events. The different location and magnitude of eruptions may certainly explain some of this heterogeneity. We show that each proxy alone cannot provide the full information of the volcanic impact on climate but that it contributes to the formation of the full picture by adding to a single, specific factor, which is critical for a comprehensive description of climate dynamics induced by volcanism and the inclusion of these phenomena in global climate models.

The analyses with a larger number of samples in the investigations of Siberian and other Northern Hemispheric sites will indeed provide higher certainty in terms of data interpretation of climatic dynamics of these boreal regions. The multi-proxy approach as applied in our study provides a strong set of complementary information to the research field, as it allows the refinement of the interpretations and thus improves our understanding of the heterogeneity of climatic signals after CE stratospheric volcanic eruptions, as recorded in multiple tree-ring and stable isotope parameters.

Author contribution: TRW analysis was performed at V.N. Sukachev Institute of Forest SB RAS by O.V. Churakova (Sidorova), D.V. Ovchinnikov, V.S. Myglan and O.V. Naumova. CWT analysis was carried out at the V. N. Sukachev Institute of Forest SB RAS, Krasnoyarsk, Russia by M. Fonti and at the University of Arizona by I. Panyushkina. Stable isotope analysis was conducted at the Paul Scherrer Institute (PSI), by O. V. Churakova (Sidorova), M. Saurer, and R. Siegwolf. MXD measurements were realized with a DENDRO Walesh 2003 densitometer at WSL and at the V.N. Sukachev Institute of Forest SB RAS, Krasnoyarsk, Russia by O. V. Churakova (Sidorova) and A. V. Kirdyanov. Samples from YAK and TAY were collected by M. M. Naurzbaev. All authors contributed significantly to the data analysis and paper writing.

Acknowledgements: This work was supported by Marie Curie International Incoming Fellowship [EU_ISOTREC 235122], Re-Integration Marie Curie Fellowship [909122] and UFZ scholarship [2006], RFBR [09-05-98015_r_sibir_a] granted to Olga V. Churakova (Sidorova); SNSF M. Saurer [200021_121838/1]; Era.Net RUSPlus project granted to M. Stoffel [SNF IZRPZ0_164735] and RFBR [№ 16-55-76012 Era_a] granted to E.A. Vaganov; project granted to Vladimir S. Myglan RNF, Russian Scientific Fond [№ 15-14-30011]; Alexander V. Kirdyanov was supported by the Ministry of Education and Science of the Russian Federation [#5.3508.2017/4.6] and RSF [#14-14-00295]; Scientific School [3297.2014.4] granted to Eugene A. Vaganov; and US National Science Foundation (NSF) grants [#9413327, #970966,

#0308525] to Malcolm K. Hughes and US CRDF grant # RC1-279, to Malcolm K. Hughes and Eugene A. Vaganov. We thank Tatjana Boettger for her support and access to the stable isotope facilities within UFZ Haale/Saale scholarship 2006; Anne Verstege, Daniel Nievergelt for their help with sample preparation for the MXD and Paolo Cherubini for providing lab access at the Swiss Federal Institute for Forest, Snow and Landscape Research (WSL).

We thank two anonymous reviewers and handling Editor Juerg Luterbacher for their constructive comments on this manuscript.

Figure legend

Fig. 1. Map with the locations of the study sites (stars) and volcanic eruptions (black dots) considered in this study (a). Annual tree-ring width index (light lines) and smoothed by 51-year Hamming window (bold lines) chronologies from northeastern Yakutia (YAK - **blue**, b) (Hughes *et al.*, 1999; Sidorova 2003), eastern Taimyr (TAY - **green**, c) (Naurzbaev *et al.*, 2002), and Russian Altai (ALT - **red**, d) (Myglan *et al.*, 2009) were constructed based on larch trees (Photos: V. Myglan – ALT, M. M. Naurzbaev – YAK, TAY).

Fig. 2. Normalized (z-score) individual tree-ring index chronologies (TRWi, **black**), maximum latewood density (MXD, **purple**), cell wall thickness (CWT, **green**), $\delta^{13}C$ (**red)** and $\delta^{18}O$ (**blue**) in tree-ring cellulose chronologies from YAK, TAY and ALT for the specific periods 10 years before and after the eruptions CE 535, 1257, 1640, 1815 and 1991 are presented. Vertical lines showed year of the eruptions.

Fig. 3. Superposed epoch analysis of $\delta^{18}O$, $\delta^{13}C$, CWT, TRW and MXD chronologies for the Yakutia (YAK), Taimyr (TAY), and Altai (ALT) sites, summarizing anomalies of the volcanic eruptions in CE 535, 540, 1257, 1640, 1815, and 1991.

Fig. 4. Significant correlation coefficients between tree-ring parameters and weather station data: temperature (**red**), precipitation (**blue**), vapor pressure deficit (**green**), and sunshine duration (yellow) from September of the previous year to August of the current year for three study sites were calculated. Table 2 lists stations used in the analysis.

Fig. 5. Response of larch trees from Siberia to the CE volcanic eruptions (Table 1) with percentile of distribution considered as very extreme (< 5th, intensive color), extreme (>5th, <10th, light color) and non-extreme (>10th, white color). July temperature changes presented as a square from **heavy blue** (cold) to **light blue** (moderate). Summer vapor pressure deficit (VPD) variabilities are shown as a circle from **purple** (low), light purple (moderate decrease) to **orange** (increase, developing to dry air). July precipitation presented as a rhomb from **heavy turquoise** (wet), **light blue** (moderate) to **orange** (dry). Low July sunshine duration shown as black triangle, while high – as yellow.

Table 1. List of stratospheric volcanic eruptions used in the study.

Table 2. Summary of tree-ring sites in northeastern Yakutia (YAK), eastern Taimyr (TAY) and Altai (ALT), and weather stations used in the study. Monthly air temperature (T, °C), precipitation (P, mm), sunshine duration (S, h/month) and vapor pressure deficit (VPD, kPa) data were used from available meteorological database http://aisori.meteo.ru/ClimateR.

References

Abaimov, A.P., Bondarev, A.I., Yzrzanova, O.V., Shitova, S.A.: Polar forests of Krasnoyarsk region. Nauka Press, Novosibirsk. 208 p, 1997.

Battipaglia, G., Cherubini, P., Saurer, M., Siegwolf, R.T.W., Strumia, S., Cotrufo, M.F.: Volcanic explosive eruptions of the Vesuvio decrease tree-ring growth but not photosynthetic rates in the surrounding forests. Global Change Biology. 13, 1-16, 2007.

Barinov, V.V., Myglan, V.S., Taynik, A.V., Ojdupaa, O.Ch., Agatova, A.R., Churakova (Sidorova) O.V. Extreme climatic events in Altai-Sayan region as indicator of major volcanic eruptions. Geophysical processes and biosphere. 17, 45-61, 2018. doi: 10.21455/GPB2018.3-3.

Beerling, D.J., Woodward, F.I.: Ecophysiological responses of plants to global environmental change since the last glacial maximum. New Phytologist. 125, 641–648, 1994.

Boettger T., Haupt, M., Knöller, K., Weise, S., Waterhouse, G.S. … Schleser, G.H.: Wood cellulose preparation methods and mass spectrometric analyses of $\delta^{13}C$, $\delta^{18}O$, and non ex-changeable $\delta^{2}H$ values in cellulose, sugar, and starch: An inter-laboratory comparison, Anal. Chem. 79, 4603–4612, doi:10.1021/ac0700023, 2007.

Boike, J., Kattenstroth, B., Abramova, K., Bornemann, N., Cherverova, A., Fedorova, I., Fröb, K., Grigoriev, M., Grüber, M., Kutzbach, L., Langer, M., Minke, M., Muster, S., Piel, K., Pfeiffer, E.-M., Stoff, G., Westermann, S., Wischnewski, K., Wille, C., Hubberten, H.-W.: Baseline characteristics of climate, permafrost and land cover from a new permafrost observatory in the Lena Rive Delta, Siberia (1998-2011). Biogeosciences. 10, 2105-2128, 2013.

Briffa, K.R., Jones, P.D., Schweingruber, F.H., Osborn, T.J.: Influence of volcanic eruptions on Northern Hemisphere summer temperature over the past 600 years. Nature. 393, 450–455, 1998.

Bryukhanova, M.V., Fonti, P., Kirdyanov, A.V., Siegwolf, R., Saurer, M., Pochebyt, N.P., Churakova (Sidorova), O.V., Prokushkin, A.S.: The response of $\delta^{13}C$, $\delta^{18}O$ and cell anatomy of *Larix gmelinii* tree rings to differing soil active layer depths. Dendrochronologia. 34, 51-59, 2015.

Büntgen, U., Myglan, V.S., Ljungqvist, F.C., McCormick, M., Di Cosmo, N., Sigl M., ….Kirdyanov, A.V.: Cooling and societal change during the Late Antique Little Ice Age from 536 to around 660 AD. Nature Geoscience. 9, 231-236, 2016.

Castagneri, D., Fonti, P., von Arx, G., Carrer, M.: How does climate influence xylem morphogenesis over the growing season? Insights from long-term intra-ring anatomy in *Picea abies*. Annals of Botany 19:1011-1020, doi:10.1093/aob/mcw274, 2017.

Cernusak, L., Ubierna, N., Winter, K., Holtum, J.A.M., Marshall, J.D., Farquhar, G.D.: Environmental and physiological determinants of carbon isotope discrimination in terrestrial Plants. Transley Review New Phytologist. 200, 950-965, 2013.

Cernusak, L., Barbour, M., Arndt, S., Cheesman, A., English, N., Field, T., Helliker, B., Holloway-Phillips, M., Holtum, J., Kahmen, A., Mcnerney F, Munksgaard N, Simonin K, Song X, Stuart-Williams H, West J and Farquhar G.: Stable isotopes in leaf water of terrestrial plants. Plant, Cell & Environment. 39 (5), 1087-1102, 2016.

Churakova (Sidorova), O.V., Bryukhanova, M., Saurer, M., Boettger, T., Naurzbaev, M., Myglan, V.S., Vaganov, E.A., Hughes, M.K., Siegwolf, R.T.W.: A cluster of stratospheric volcanic eruptions in the AD 530s recorded in Siberian tree rings. Global and Planetary Change. 122, 140-150., 2014.

Churakova (Sidorova), O.V., Shashkin, A.V., Siegwolf, R., Spahni, R., Launois, T., Saurer M., Bryukhanova, M.V., Benkova, A.V., Kupzova, A.V., Vaganov, E.A., Peylin, P., Masson-Delmotte, V., Roden, J.: Application of eco-physiological models to the climatic interpretation of $\delta^{13}C$ and $\delta^{18}O$ measured in Siberian larch tree-rings. Dendrochronologa, doi:10.1016/j.dendro.2015.12.008, 2016.

Cook, E., Briffa, K., Shiyatov, S., Mazepa, V.: Tree-ring standardization and growth trend estimation. In: Methods of dendrochronology: applications in the environmental sciences, Eds: Cook, E.R., Kairiukstis, L.A. 104-123, 1990.

Cook, E.R., Krusic, P.J.: A Tree-Ring Standardization Program Based on Detrending and Autoregressive Time Series Modeling, with Interactive Graphics (ARSTAN). (Ed. by E.R., Cook and P.J., Krusic), 2008.

Craig, H.: Isotopic variations in meteoric waters. Science. 133, 1702– 1703, 1961.

Crowley, T.J., Unterman, M.B.: Technical details concerning development of a 1200 yr. proxy index for global volcanism. Earth Syst. Sci. Data. 5, 187-197, 2013.

Cuny, H.E., Rathgeber, C.B.K., Frank, D., Fonti, P., Fournier, M.: Kinetics of tracheid development explain conifer tree-ring structure. New Phytologist, 203, 1231–1241, 2014.

D'Arrigo, R.D., Jacoby, G.C., Frank, D., Pederson, N.D., Cook, E., Buckly, B.M., Nachin, B., Mijidorj, R., Dugarjav, C.: 1738-years of Mongolian temperature variability inferred from a tree-ring width chronology of Siberian pine. Geophisycal Research Letters. Vol. 28 (3), 543-546, 2001.

Dansgaard, W.: Stable isotopes in precipitation. Tellus. 16, 436–468, 1964.

Dawson, T.E., Mambelli, S., Plamboeck, A.H., Templer, P.H., Tu, K.P.: Stable isotopes in plant ecology Ann. Review of Ecology and Systematics. 33, 507-559, 2004.

Dongmann, G., Förstel, H., Wagener, K.: ^{18}O-rich oxygen from land photosynthesis. Nature New Biol. 240, 127–128, 1972.

Eschbach, W., Nogler, P., Schär, E., Schweingruber, F.H.: Technical advances in the radiodensitometrical determination of wood density. Dendrochronologia. 13, 155–168, 2015.

Esper, J., Büntgen, U., Hartl-Meier, C., Oppenheimer, C., Schneider, L.: Northern Hemisphere temperature anomalies during 1450s period of ambiguous volcanic forcing. Bull. Volcanology. 79, 41, 2017.

Farquhar, G. D.: Eds. Stable Isotopes and Plant Carbon-Water Relations. Academic Press, San Diego. 47–70, 1982.

Farquhar, G.D., Ehleringer, J.R., Hubick, K.T.: Annu. Rev. Plant Physiol. Plant Mol. Biol. 40, 503 p, 1989.

Farquhar, G.D., Lloyd, J.: Carbon and oxygen isotope effects in the exchange of carbon dioxide between terrestrial plants and the atmosphere. In: Ehleringer, J.R., Hall, A.E., Farquhar, G.D. (Eds) Stable Isotopes and Plant Carbon-Water Relations. Academic Press, San Diego, 47–70, 1993.

Fonti, P., Bryukhanova, M.V., Myglan, V.S., Kirdyanov, A.V., Naumova, O.V., Vaganov, E.A.: Temperature-induced responses of xylem structure of *Larix sibirica* (Pinaceae) from Russian Altay. American Journal of Botany. 100 (7), 1-12, 2013.

Francey, R.J., Allison, C.E., Etheridge D.M., Trudinger, C.M., Langenfelds, R.L., Michel, E., Steele, L.P.: A 1000-year high precision record of $\delta^{13}C$ in atmospheric CO_2. Tellus. Ser. B (51), 170-193, 1999.

Fritts, H.C.: Tree-rings and climate. London. New York; San Francisco: Acad. Press. 567 p, 1976.

Furst, G.G.: Methods of Anatomical and Histochemical Research of Plant Tissue. Nauka, Moscow. 156 p, 1979.

Gao, C., Robock, A., Ammann, C.: Volcanic forcing of climate over the past 1500 years: An improved ice core-based index for climate models. J. Geophys. Res. Atmos. 113:D23111. doi:10.1029/2008jd010239, 2008.

Gennaretti, F., Huard, D., Naulier, M., Savard, M., Bégin, C., Arseneault, D., Guiot, J.: Bayesian multiproxy temperature reconstruction with black spruce ring widths and stable isotopes from the northern Quebec taiga. Clym. Dyn. doi: 10.1007/s00382-017-3565-5, 2017.

Gillett, N.P., Weaver, A.J., Zwiers, F.W. Wehner, M.F.: Detection of volcanic influence on global precipitation. Geophysical Research Letters, 31 (12), doi:10.1029/2004GL020044 R, 2004.

Groisman, P.Ya.: Possible regional climate consequences of the Pinatubo eruption. Geophys. Res. Lett., 19, 1603–1606, 1992.

Gu, L., Baldocchi, D.D., Wofsy, S.C., Munger, J.W., Michalsky, J.J., Urbanski, S.P., Boden, T.A.: Response of a deciduous forest to the Mount Pinatubo eruption: Enhanced photosynthesis, Science. 299 (5615), 2035–2038, 2003.

Guillet, S., Corona, C., Stoffel, M., Khodri M,, Lavigne F., Ortega, P.,….Oppenheimer, C.: Climate response to the 1257 Samalas eruption revealed by proxy records. Nature geoscience, doi:10.1038/ngeo2875, 2017.

Hansen, J., Sato, M., Ruedy, R., Lacis, A., Asamoah, K., Borenstein S,, ….Wilson, H.: A Pinatubo climate modeling investigation. In The Mount Pinatubo Eruption: Effects on the Atmosphere and Climate, NATO ASI Series Vol. I 42. G. Fiocco, D. Fua, and G. Visconti, Eds. Springer-Verlag, 233-272, 1996.

Harrington, C.R.: The Year without a summer? World climate in 1816. Ottawa: Canadian Museum of Nature, ISBN 0660130637, 1992.

Helama, S., Arppe, L., Uusitalo, J., Holopainen, J., Mäkelä, H.M., Mäkinen, H., Mielikäinen, K., Nöjd, P., Sutinen, R., Taavitsainen, J.-P., Timonen, M., Oinonen, M.: Volcanic dust veils from sixth century tree-ring isotopes linked to reduced irradiance, primary production and human health. Scientific reports 8, 1339, doi:10.1038/s41598-018-19760-w, 2018.

Hughes, M.K., Vaganov, E.A., Shiyatov, S.G., Touchan, R. & Funkhouser, G.: Twentieth-century summer warmth in northern Yakutia in a 600-year context. The Holocene. 9(5), 603-608, 1999.

Iles, C.E., Hegerl, G.C.: The global precipitation response to volcanic eruptions in the CMIP5 models. Environ. Res. Lett. 9, doi:10.1088/1748-9326/9/10/104012, 2014.

Joseph, R., Zeng, N.: Seasonally modulated tropical drought induced by volcanic aerosol. J. Climate, 24, 2045–2060, 2011.

Kirdyanov, A.V., Treydte, K.S., Nikolaev, A., Helle, G., Schleser, G.H.: Climate signals in tree-ring width, wood density and $\delta^{13}C$ from larches in Eastern Siberia (Russia) Chemical Geology, 252, 31-41, 2008. doi:10.1016/j.chemgeo.2008.01.023

Körner, Ch.: Paradigm shift in plant growth control. Curr. Opinion Plant Biol. 25, 107-114, 2015.

Lavigne, F., Degeai, J.-P., Komorowski, J.-C., Guillet, S., Robert, V., Lahitte, P., Oppenheimer, C., Stoffel, M., Vidal, C.M., Suro, I.P., Wassmer, P., Hajdas, I., Hadmoko, D.S., Belizal, E.: Source of the great A.D. 1257 mystery eruption unveiled, Samalas volcano, Rinjani Volcanic Complex, Indonesia. Proc Natl Acad Sci 110, 16742–16747, doi:10.1073/pnas.1307520110, 2013.

Lehmann, M.M., Goldsmith, G.T., Schmid, L., Gessler, A., Saurer, M., Siegwolf, R.T.W.: The effect of ^{18}O-labelled water vapour on the oxygen isotope ratio of water and assimilates in plants at high humidity. New Phytologist. 217, 1, 105-116. doi: 10.1111/nph.14788, 2018.

Lenz, O., Schär, E., Schweingruber F.H.: Methodische Probleme bei der radiographisch-densitometrischen Bestimmung der Dichte und der Jahrrinbreiten von Holz. Holzforschung, 30, 114-123, 1976.

Loader, N.J., Robertson, I., Barker, A.C., Switsur, V.R., Waterhouse, J.S.: Improved technique for the batch processing of small whole wood samples to alpha-cellulose. Chemical Geology. 136, 313-317, 1997.

Loader, N.J., Young, G.H.F., Grudd, H., McCarroll.: Stable carbon isotopes from Torneträsk, norther Sweden provide a millennial length reconstruction of summer sunshine and its relationship to Arctic circulation. Quaternary Science Reviews. 62, 97-113, 2013.

McCarroll, D., Loader, N.J.: Stable isotopes in tree rings. Quaternary Science Review. 23, 771-801, 2004.

Meronen, H., Henriksson, S.V., Räisänen, P., Laaksonen, A.: Climate effects of northern hemisphere volcanic eruptions in an Earth System Model. Atmospheric Research, 114-115: 107-118, 2012.

Munro, M.A.R., Brown, P.M., Hughes, M.K., Garcia, E.M.R.: Image analysis of tracheid dimensions for dendrochronological use. Radiocarbon, Eds. by M.D. Dean, J. Swetnam T), pp. 843-851. Tucson, Arizona, 1996.

Myglan, V.S., Oidupaa, O. Ch., Kirdyanov, A.V., Vaganov, E.A.: 1929-year tree-ring chronology for Altai-Sayan region (Western Tuva). Journal of archeology, ethnography and anthropology of Eurasia. 4 (36), 25-31, 2008.

Naurzbaev, M.M., Vaganov, E.A., Sidorova, O.V., Schweingruber, F.H.: Summer temperatures in eastern Taimyr inferred from a 2427-year late-Holocene tree-ring chronology and earlier floating series. The Holocene. 12(6), 727-736, 2002.

Panofsky, H.A., Brier, G.W.: Some applications of statistics to meteorology. University Park, PA. Mineral industries extension services, college of mineral industries, Pennsylvania State University, 224 p, 1958.

Panyushkina, I.P., Hughes, M.K., Vaganov, E.A., Munro, M.A.R.: Summer temperature in northern Yakutia since AD 1642 reconstructed from radial dimensions of larch tracheids. Canadian Journal of Forest Research. 33, 1-10, 2003.

Peng, Y., Shen, C., Wang, W.-C., Xu, Y.: Response of summer precipitation over Eastern China to large volcanic eruptions. Journal of Climate. 23, 818-824, 2009.

R Core Team.: R: A Language and Environment for Statistical Computing. Vienna, Austria, 2016.

Robock, A.: Volcanic eruptions and climate. Reviews of Geophysics. 38(2), 191-219, 2000.

Robock, A., Liu, Y.: The volcanic signal in Goddard Institute for Space Studies three-imensional model simulations. J. Climate. 7, 44-55, 1994.

Roden, J.S., Siegwolf, R: Is the dual isotope conceptual model fully operational? Tree Physiology. 32, 1179-1182, 2012.

Saurer, M., Kirdyanov, A.V., Prokushkin, A.S., Rinne K.T., Siegwolf, R.T.W.: The impact of an inverse climate–isotope relationship in soil water on the oxygen-isotope composition of *Larix gmelinii* in Siberia. New Phytologist. 109, 3, 955-964, 2016.

Saurer, M., Robertson, I., Siegwolf, R., Leuenberger, M.: Oxygen isotope analysis of cellulose: an interlaboratory comparison. Analytical cemistry, 70, 2074-2080, 1998.

Saurer, M., Kirdyanov, A. V., Prokushkin, A. S., Rinne, K. T., Siegwolf, R.T.W.: The impact of an inverse climate-isotope relationship in soil water on the oxygen-isotope composition of *Larix gmelinii* in Siberia. New Phytologist. 209(3), 955-964, 2016.

Scheidegger, Y., Saurer, M., Bahn, M., Siegwolf, R.: Linking stable oxygen and carbon isotopes with stomatal conductance and photosynthetic capacity: a conceptual model. Oecologia. 125, 350–357. doi: 10.1007/s004420000466, 2000.

Schneider, L., Smerdon, J.E., Büntgen, U., Wilson, R.J.S., Myglan, V.S., Kirdyanov, A.V., Esper, J.: Revising mid-latitude summer temperatures back to A.D. 600 based on a wood density network. Geophys. Res. Lett. 42, GL063956, doi:10.1002/2015gl063956, 2015.

Schweingruber, F.H.: Tree rings and environment dendroecology. Paul Haupt Publ Bern, Stuttgart, Vienna 1996. pp. 609, 1996.

Sidorova, O.V., Naurzbaev, M.M.: Response of Larix cajanderi to climatic changes at the upper timberline and in the Indigirka River valley. Lesovedenie (in Russian). 2, 73-75, 2002.

Sidorova, O.V.: Long-term climatic changes and the larch radial growth on the northern Middle Siberia and the Northeastern Yakutia in the Late Holocene. Abs. PHD Diss, V.N. Sukachev Institute of Forest, Krasnoyarsk, 2003.

Sidorova, O.V., Naurzbaev, M.M., Vaganov, E.A.: Response of tree-ring chronologies growing on the Northern Eurasia to powerful volcanic eruptions. Problems of ecological monitoring and ecosystem modeling, XX, 60-72, 2005.

Sidorova, O.V., Saurer, M., Myglan, V.S., Eichler, A., Schwikowski, M., Kirdyanov, A.V., Bryukhanova, M.V., Gerasimova, O.V., Kalugin, I., Daryin, A., Siegwolf, R.:. A multi-proxy approach for revealing recent climatic changes in the Russian Altai. Climate Dynamics, 38 (1-2), 175–188, 2011.

Sidorova, O.V., Siegwolf, R., Myglan, V.S., Loader, N.J., Helle, G., Saurer, M.: The application of tree-rings and stable isotopes for reconstructions of climate conditions in the Altai-Sayan Mountain region. Climatic Changes, doi: 10.1007/s10584-013-0805-5, 2012.

Sidorova, O.V., Siegwolf, R., Saurer, M., Naurzbaev, M., Shashkin, A.V., Vaganov, E.A.: Spatial patterns of climatic changes in the Eurasian north reflected in Siberian larch tree-ring parameters and stable isotopes. Global Change Biology, doi: 10.1111/j.1365-2486.2009.02008.x, 16, 1003-1018, 2010.

Sidorova, O.V., Siegwolf, R.T.W., Saurer, M., Naurzbaev, M.M., Vaganov, E.A.: Isotopic composition ($\delta^{13}C$, $\delta^{18}O$) in Siberian tree-ring chronology. Geophysical research Biogeosciences. 113, 1-13, 2008.

Sigl, M., Winstrup, M., McConnell, J.R.: Timing and climate forcing of volcanic eruptions for the past 2500 years. Nature. 523, 543-549. doi:10.1038/nature14565, 2015.

Sprenger, M., Tetzlaff, D., Buttle, J. M., Laudon, H., Leistert, H., Mitchell, C., Snelgrove, J., Weiler, M., Soulsby, C.: Measuring and modelling stable isotopes of mobile and bulk soil water, Vadose Zone Journal, https://doi.org/10.2136/vzj2017.08.0149, 20, 2017.

Sternberg, L.S.O.: Oxygen stable isotope ratios of tree-ring cellulose: The next phase of understanding. New Phytologist. 181 (3), 553-562, 2009.

Stirzaker, D.: Elementary Probability density functions. Cambridge. Sec. Ed. 538 p, 2003.

Stoffel, M., Khodri, M., Corona, C., Guillet, S., Poulain, V., Bekki, S., Guiot, J., Luckman, B.H., Oppenheimer, C., Lebas, N., Beniston, M., Masson-Delmotte, V.: Estimates of volcanic-induced cooling in the Northern Hemisphere over the past 1,500 years. Nature Geoscience. 8, 784–788, 2015.

Stothers, R.B.: Climatic and Demographic Consequences of the Massive Volcanic Eruption of 1258. Climatic Change. 45, 361-374, 2000.

Stothers, R.B.: Mystery cloud of AD 536. Nature. 307, 344-345, doi:10.1038/307344a0, 1984.

Sugimoto, A., Yanagisawa, N., Fujita, N., Maximov, T.C.: Importance of permafrost as a source of water for plants in east Siberian taiga. Ecological Research. 17 (4), 493-503, 2002.

Toohey, M., Sigl, M.: Volcanic stratospheric sulphur injections and aerosol optical depth from 500 BCE to 1900 CE. Earth System Science Data. doi:10.5194/essd-9-809-2017, 2017.

Vargas, A. I., Schaffer, B, Yuhong, L. Sternberg, L.S.: Testing plant use of mobile vs immobile soil water sources using stable isotope experiments. New Phytologist. 215, 582–594, doi: 10.1111/nph.14616, 2017.

Vaganov, E.A., Hughes, M.K., Kirdyanov, A.K., Schweingruber, F.H., Silkin, P.P.: Influence of snowfall and melt timing on tree growth in subarctic Eurasia. Nature. 400, 149-151, 1999.

Vaganov, E.A., Hughes, M.K., Shashkin, A.V.: Growth dynamics of conifer tree rings. Springer Verlag, Berlin., pp. 353, 2006.

Wegmann, M., Brönnimann, S., Bhend, J., Franke, J., Folini, D., Wild, M., Luterbacher, J.: Volcanic influence on European summer precipitation through monsoons: Possible cause for "years without summer". AMS, doi.org/10.1175/JCLI-D-13-00524.1, 2014.

Wigley, T.M.L., Briffa, K.R., Jones, P.D.: On the Average Value of Correlated Time Series, with Applications in Dendroclimatology and Hydrometeorology. Journal of Climate and Applied Meteorology. 23 (2), 201-213, doi:10.1175/15200450(1984)023.0201, 1984.

Wiles, G.C., D'Arrigo, R.D., Barclay, D., Wilson, R.S., Jarvis, S.K., Vargo, L., Frank, D.: Surface air temperature variability reconstructed with tree rings for the Gulf of Alaska over the past 1200 years. The Holocene. 6, 10.1177/0959683613516815, 2014.

Wilson, R.J.S., Anchukaitis, K., Briffa, K. et al.: Last millennium Northern Hemisphere summer temperatures from tree rings. Part I: the long-term context. Quaternary Science Review. 134, 1–18, 2016.

Zielinski, G.A., Mayewski, P.A., Meeker, L.D., Whitlow, S., Twickler, M.S., Morrison, M., Meese, D.A., Gow A.J., Alley, R.B.: Record of volcanism since 7000 BC from the GISP2 Greenland ice core implications for the volcano-climate system. Science. 264 (5161), 948-952, 1994.